Vibrational Relaxation and Hydrogen-Bond Dynamics of HDO:H_2O

Michel F. Kropman,* Han-Kwang Nienhuys, Sander Woutersen, and Huib J. Bakker

FOM Institute for Atomic and Molecular Physics, Kruislaan 407, 1098 SJ Amsterdam, The Netherlands

Received: January 5, 2001

Femtosecond two-color mid-infrared pump−probe spectroscopy is used to study the vibrational relaxation and the hydrogen-bond dynamics of HDO dissolved in liquid H_2O. By looking at the spectral dynamics of the OD stretch mode, direct information on the hydrogen-bond dynamics of the H_2O solvent is obtained. By fitting the data using the Brownian oscillator model, we determined the vibrational lifetime of the OD stretch vibration and the hydrogen-bond length correlation time. The hydrogen-bond correlation time of H_2O is significantly shorter than for D_2O, found previously.

1. Introduction

Infrared and Raman spectroscopy have long been used to study liquid water.[1,2] Unfortunately, these conventional linear spectroscopic techniques do not give information on the dynamics of the water molecules because, due to the large variation in hydrogen-bond lengths, the vibrational absorption bands are strongly inhomogeneously broadened. Advancements in laser technology have enabled the use of nonlinear spectroscopic techniques. However, to probe dynamical behavior with these techniques, the pulse duration has to be shorter than the time scale of the phenomenon under consideration.

The vibrational modes in water are optically active in the mid-infrared.[3] At these wavelengths, no laser sources are available that deliver short and powerful pulses. Using frequency-conversion processes[4] in nonlinear crystals such as $LiNbO_3$, the available wavelengths (e.g., 1064 nm for Nd:YAG lasers or 800 nm for Ti:sapphire lasers) can be converted into mid-infrared light. This conversion requires a high-intensity source laser; the experiments that can be performed are thus limited by the pulse duration and energy of the pulses of the source laser.

In the 1970s, Nd:glass[5] and Nd:YAG[6] lasers were developed, producing powerful picosecond pulses, typically 1 mJ and 6 ps for Nd:glass, and 40 mJ and 20 ps for Nd:YAG. The lasers had a fairly low repetition rate, 10 Hz for Nd:YAG and only 1 Hz for Nd:glass, which made it very difficult to obtain data within an acceptable signal-to-noise ratio. Nevertheless, with these lasers it became possible to study the dynamics of vibrational excitations in monomers such as hydrogen chloride (HCl)[6] and chloroform ($CHCl_3$),[7] and ethanol clusters (C_2H_5OH)[8] dissolved in carbon tetrachloride (CCl_4). With the advent of Ti:sapphire lasers, that produce powerful subpicosecond laser pulses at a 1 kHz repetition rate, the study of faster processes occurring in hydrogen-bonded species such as liquid water[9−14] and ethanol[15] came within reach.

The study of water is complicated by the hydrogen-bond structure, and by the strong coupling between OH groups of neighboring molecules.[13,14] Furthermore, the symmetric and antisymmetric stretching vibrations in liquid H_2O are spectroscopically nearly indistinguishable. To avoid these complications, experimental work has mainly been devoted to dilute solutions of HDO in D_2O,[1,9,11,12,16] where the OH and OD stretching bands are well separated, being centered at 3400 and 2500 cm^{-1}, respectively, while the chemical (hydrogen-bonded) structure remains nearly unchanged.

Using femtosecond mid-infrared pump−probe spectroscopy, it was shown that the OH stretching vibration of HDO in D_2O has a lifetime of approximately 740 fs.[12,14] In other studies, the hydrogen-bond dynamics was studied by looking at the time-dependent signal at frequencies different from the excitation frequency.[11,16] It was found that the OH stretching frequency, and therefore the hydrogen-bond length, is not constant in time, but rather changes on a time-scale of approximately 500 fs. These hydrogen-bond dynamics, however, are determined by the D_2O "solvent". To study the hydrogen-bond dynamics of H_2O ("real water"), we would like to probe the OH stretching vibration in pure H_2O. Unfortunately, as a result of rapid intermolecular energy transfer,[13,14] the OH stretching vibration is not localized on one OH oscillator for a sufficient period of time. Therefore, it is not possible to obtain information on the hydrogen-bond dynamics of liquid water by probing the OH stretch in pure H_2O. However, by looking at the OD stretching vibration of HDO in H_2O, information on these dynamics can be obtained.

2. Experiment

To perform time-resolved two-color pump−probe spectroscopy on the OD stretching vibration, we need powerful femtosecond pump and probe pulses at wavelengths near 4000 nm. The pump pulses are generated using the setup shown in Figure 1. A commercial Ti:sapphire regenerative/multipass amplifier delivers pulses of 800 nm wavelength, 3 mJ energy, 100 fs duration, at a 1 kHz repetition rate. Part of this 800 nm light (0.9 mJ) is used to pump an optical parametric generation and amplification stage (OPA) based on β-barium borate (BBO), that can be tuned from 1.1 to 2.6 μm. In our experiment, it is tuned to approximately 1330 nm (signal) and 2000 nm (idler). The idler is subsequently frequency-doubled to 1000 nm using a second BBO crystal. The 1000 nm light is used as seed in a second parametric amplification process, where it is combined with a fresh part (1.4 mJ) of the 800 nm light in a 5 mm potassium niobate ($KNbO_3$) crystal to produce 4000 nm (2500 cm^{-1}) pulses. Residual seed and pump light is filtered out of the beam using dielectric 800 nm and YAG mirrors, and a long

* To whom correspondence should be addressed. E-mail: m.kropman@amolf.nl.

10.1021/jp010057n CCC: $20.00
Published on Web 04/20/2001

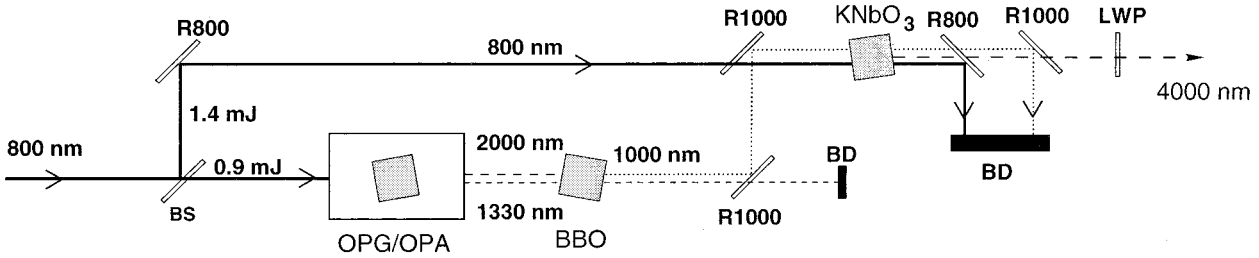

Figure 1. Generation of 4 μm pump pulses. Abbreviations: BBO, $KNbO_3$: crystals; R800, R1000: dielectric 800 nm, broadband 900−1100 nm mirrors; LWP: long wave pass-filter, BD: beam dump, OPG/OPA: 3-pass optical parametric generation and amplification stage based on BBO.

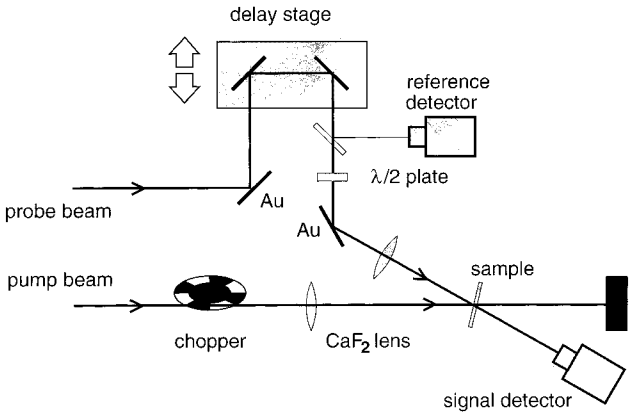

Figure 2. Pump−probe setup. The signal detector measures the total intensity of the delayed probe pulse, divided by the intensity measured by the refererence detector, to account for the pulse-to-pulse intensity variations. The chopper blocks every other pump pulse, to obtain the pump-induced absorption change of the sample. Gold mirrors and CaF_2 plates and lenses are used to direct and focus the beams. A $\lambda/2$ plate rotates the probe beam polarization to exclude effects of reorientation.

wave pass filter. By tuning the seed pulses, the output pulses are tuned from 3700 to 4250 nm (2350−2700 cm^{-1}), with a typical energy of 18 μJ, and a bandwidth of 70 nm.

The probe pulses at wavelengths below 4250 nm are generated nearly the same way. A second OPA based on a BBO crystal is pumped with 0.4 mJ 800 nm pulses. Its output at 2000 nm is converted into 1000 nm using a second BBO crystal. For the mid-infrared generation, we now use $LiNbO_3$, since with this crystal the spectral shape and pulse energy of the generated light are more stable than with a $KNbO_3$ crystal. It is pumped with 0.1 mJ 800 nm light. Cross-correlation traces of these pulses with the pump pulses (delay-dependence of sum-frequency generation in a $LiIO_3$ crystal), have a fwhm of 350 fs (pulse duration of 250 fs).

Because of the absorbance in $LiNbO_3$ at longer wavelengths, we use a different method to generate (probe) wavelengths longer than 4250 nm. The OPA is now pumped with 0.6 mJ of 800 nm light. For the generation of the 4400 nm pulses used in the present experiment, it is tuned to 1350 (signal) and 1950 nm (corresponding idler). In a 3 mm $AgGaS_2$ crystal, signal and idler are used in a difference-frequency generation process. Cross-correlation traces of these pulses have a fwhm of 600 fs.

The pump and probe pulses are used in a pump−probe setup, shown in Figure 2. The pump excites a significant fraction of the molecules, causing an absorption change that is measured by the probe beam. The absorption will decrease when the probe is tuned to some frequency within the $0 \rightarrow 1$(the numbers refer to vibrational levels) absorption band, and increase for frequencies in the $1 \rightarrow 2$ band (due to the anharmonicity of the OD stretching potential function, the $1 \rightarrow 2$ transition is red-shifted by approximately 200 cm^{-1} with respect to the $0 \rightarrow 1$ transition).

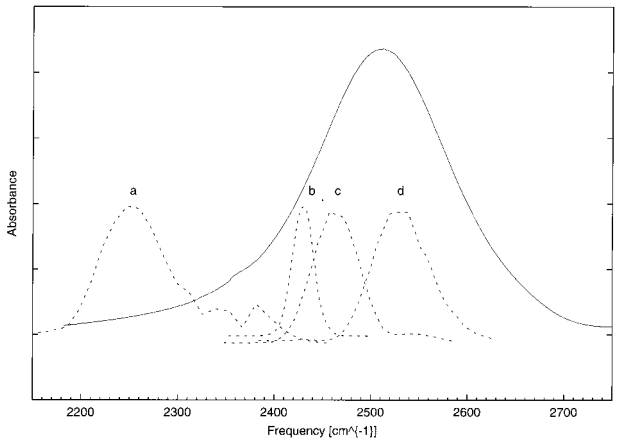

Figure 3. Absorption band of the OD stretching vibration in HDO:H_2O, corrected for the H_2O background (solid line). Also shown are the power spectra of the probe pulses used in the experiments (dotted lines; the letters correspond to the ones in Figure 4).

Part of the probe beam is split off using a CaF_2 plate and measured by a reference detector, to account for the pulse-to-pulse variations in probe energy. The pump and probe beams are focused in the sample using +175 mm and +100 mm CaF_2 lenses, respectively; the focal lengths differ to ensure that the probe beam focus is smaller than the focus of the pump. The intensities of the transmitted probe pulses and of the reference pulses are measured by PbSe detectors. A chopper is placed in the pump beam, blocking every other pump pulse. In this way, the transmitted probe pulse intensity can be measured with (I) or without the pump pulse (I_0). The transmission T of the probe beam with (without) pump beam is then given by I/I_{ref} (I_0/I_{ref}). The absorption change, $\Delta\alpha = -\ln(T/T_0)$ can now be measured as a function of the time delay between pump and probe. The polarization of the probe beam, originally parallel to the pump beam, is rotated over the magic angle (54.7°) to exclude effects of reorientation.

The sample used was a 50 μm thick layer of about 5% HDO in H_2O. Sample thickness and concentration were chosen such that the transmission at the center of the OD absorption band was approximately 5%. During the measurements, the sample was continuously rotated to avoid heating effects due to previous pulses.

3. Results

The absorption band of the OD stretching vibration is centered at 2500 cm^{-1} and has a fwhm of 170 cm^{-1} (see Figure 3). To investigate the relaxation of the OD stretching vibration, we recorded delay scans at different pump and probe frequencies. They are shown in Figure 4, where the absorption change ($\ln(T/T_0)$) is plotted as a function of the time delay between the pump and probe pulses, for several pump and probe frequencies. It is observed that the pump−probe signal strongly depends on the employed frequencies.

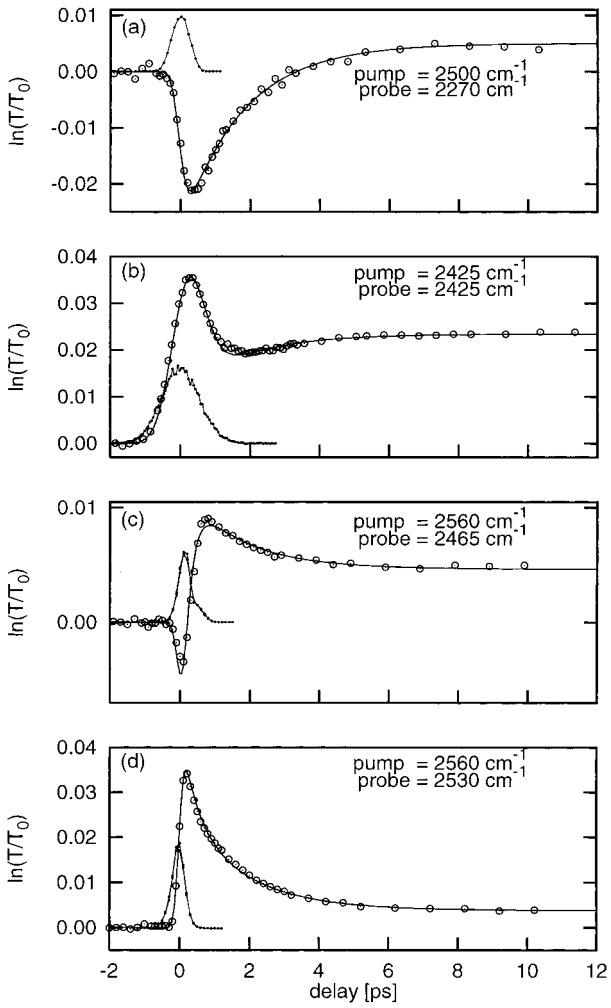

Figure 4. Measured pump−probe transients of HDO:H_2O at different pump and probe frequencies. The solid line is a fit to the data (see Section 4). Also shown are cross-correlation traces of the pump and probe pulses.

At delays shorter than 1 ps, very complex behavior is observed: in Figures 4b and 4d, a bleaching signal is observed; Figure 4a shows an induced absorption due to the $1 \rightarrow 2$ transition. In Figure 4c, within 1 ps, the initial absorption changes to a bleaching signal. After 1 ps, all signals either increase (Figures 4a and 4b) or decrease (Figures 4c and 4d) exponentially to a decreased absorption level at the same time scale of ~2 ps.

The persistent absorption change at large delays is due to the temperature increase that results from the thermalization of the pump pulse energy. Raising the temperature causes the absorption band to shift to the blue and become weaker.[17] This gives rise to an absorption decrease at most frequencies, except at high frequencies, where a final absorption increase is observed (not shown).

4. Model

The short-time behavior, within 1 ps, depends strongly on both pump and probe frequencies. For instance, the initial absorption at a 2465 cm^{-1} probe frequency (Figure 4c) is not observed when pumping at 2465 or 2500 cm^{-1}, instead of 2560 cm^{-1}. The bleaching at 2425 cm^{-1} (Figure 4b) is not observed when pumping at 2560 cm^{-1}; with this combination of pump and probe frequencies, an induced absorption signal is observed. Because of the dependence of the fast signal on both pump and probe frequencies, we assign it to a spectral diffusion process, as will be explained below. In contrast, the sign of the slow component only depends on the probe, and not on the pump frequency. This means that for the slow component (i.e., after 1 ps), the spectral diffusion has completed, so that the slow component corresponds to the actual lifetime of the vibration.

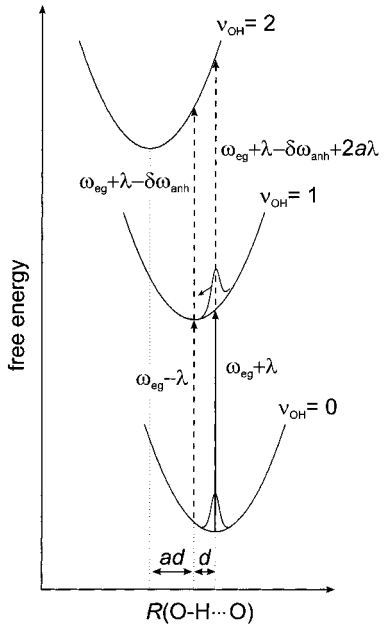

Figure 5. Harmonic potential energy functions for the OD stretching vibration (ground state and the first two excited states), as a function of the O—H···O-distance (see Section 4). $\omega_{eg} + \lambda$ is the ground-state absorption center frequency, 2λ the Stokes shift, $\delta\omega_{anh}$ the anharmonic frequency shift; d is the displacement of the potential minimum between $\nu_{OH} = 0$ and $\nu_{OH} = 1$; ad is the displacement of the minima of $\nu_{OH} = 1$ and $\nu_{OH} = 2$.

In our experiment, the pump pulse selectively excites the OD stretching vibration of a subset of the HDO molecules. The subset is characterized by a small range of OD stretching frequencies (corresponding to a particular range of hydrogen-bond lengths[18]). The $\nu = 1$ state is thus populated, and the ground-state depleted, which will change the absorbance at several frequencies. Due to the random motion of the solvent water molecules, the spectral shapes of both ground-state depletion ("holes") and excited-state population ("particles") will broaden and shift toward their respective equilibrium band shapes (spectral diffusion). Excited molecules will after some time (lifetime T_1) relax to the ground state, thereby locally raising the temperature, which results in a weakening and blueshift of the absorption band.

All the above features are incorporated in the Brownian oscillator model, that describes the time-dependent two-color pump−probe signal of a high-frequency molecular vibration coupled to a strongly damped, harmonic, low-frequency hydrogen-bond mode. For an excited OH stretching vibration, the hydrogen-bond potential is shifted over a distance d to shorter hydrogen-bond lengths compared to the potential in the vibrational ground state (see Figure 5). Thus, when the OH stretch mode is excited, the hydrogen bond will contract, and the OH stretch frequency will show a dynamical Stokes shift to lower frequencies. The relation between the absorption band shape $e^{-\omega^2/2\Delta^2}$ and the Stokes shift 2λ is given by[19]

$$2\lambda = \hbar\Delta^2/k_B T \qquad (1)$$

The hydrogen-bond mode in liquid water is strongly over-

damped. Therefore, its motion is diffusive, and can be described by a correlation function (in terms of the oscillation frequency) of the form

$$\langle \delta\omega(\tau)\delta\omega(0)\rangle = \Delta^2 e^{-\tau/\tau_c} \tag{2}$$

in which τ_c is the spectral diffusion correlation time, and Δ the root-mean-squared amplitude of the frequency fluctuations.

For the pump−probe signal, a formula can be derived giving the time-dependent absorption change as a function of pump and probe frequency.[19,20] We have added a term to account for the excited-state absorption and an overall factor of $\exp(-\tau/T_1)$ for the finite lifetime of the excitation. Another term was added to describe the effect of temperature increase on the pump−probe signal; it was simply taken proportional to the fraction of the molecules that have decayed from the $\nu = 1$ state, after which the vibrational energy has become thermal. The first three terms describe the particle, hole, and induced absorption contributions, respectively. The fourth term represents the temperature-induced absorption change.

$$S_{PP}(\omega_1, \omega_2, \tau) = F(\tau)\,\{S_p(\tau) + S_h(\tau) + S_{ea}(\tau)\} + S_T(\tau) \tag{3}$$

where

$$F(\tau) = \frac{2\pi e^{-\tau/T_1}}{\sqrt{(\Delta^2 + w_1^2)\alpha^2(\tau)}}\, e^{-(\omega_1-\omega_{eg}^0-\lambda)^2/2(\Delta^2+w_1^2)}$$

$$S_p(\tau) = e^{-(\omega_2-\omega_e(\tau))^2/2\alpha^2(\tau)}$$

$$S_h(\tau) = e^{-(\omega_2-\omega_g(\tau))^2/2\alpha^2(\tau)}$$

$$S_{ea}(\tau) = \sigma_{ea} e^{-(\omega_2-\omega_{ea}(\tau))^2/2a^2\alpha^2(\tau)} \tag{4}$$

$$S_T(\tau) = \Delta\sigma(\omega_2)\,(1 - e^{-\tau/T_1}) \tag{5}$$

$$\omega_e(\tau) = \omega_{eg}^0 - \lambda + e^{-\tau/\tau_c}\,(\omega_0 - \omega_{eg}^0 + \lambda)$$

$$\omega_g(\tau) = \omega_{eg}^0 + \lambda + e^{-\tau/\tau_c}\,(\omega_0 - \omega_{eg}^0 - \lambda)$$

$$\omega_{ea}(\tau) = \omega_{eg}^0 + \lambda - \delta\omega_{anh} + ae^{-\tau/\tau_c}\,(\omega_0 - \omega_{eg}^0 + \lambda) \tag{6}$$

$$\omega_0 = \omega_1 \frac{\Delta^2}{\Delta^2 + \omega_1^2} + (\omega_{eg}^0 + \lambda)\frac{w_1^2}{\Delta^2 + w_1^2}$$

$$\alpha^2(\tau) = \Delta^2\left[1 - \frac{\Delta^2}{\Delta^2 + w_1^2} e^{-2\tau/\tau_c}\right] + w_2^2 \tag{7}$$

ω_1, w_1 and ω_2, w_2 are the central frequencies and the spectral widths of the Gaussian pump and probe pulses, respectively. $\omega_{eg} + \lambda$ is the center frequency of the absorption band. ω_e and ω_g denote the time-dependent center frequencies of the particle and hole distributions.

All data can be described by eq 3, convolved with the cross-correlation trace, using a T_1 of 1.8 ps, a spectral diffusion correlation time of 400 fs, central frequencies of 2520 and 2350 cm^{-1}, and widths of 170 cm^{-1} and 240 cm^{-1} for the $0 \rightarrow 1$ and $1 \rightarrow 2$ transitions, respectively. The cross-section ratio σ_{ea} of the excited-state absorption relative to the ground-state absorption was found to be 1.38.

The fit results are shown in Figure 4 as solid lines. It is seen that all results are well described, including Figures 4b and 4c, that are rich in features. Pumping at the red side of the absorption band, 2425 cm^{-1} (Figure 4b), leads to a population in the $\upsilon = 1$ state, and a depletion of the ground state, that are both centered at the short-hydrogen-bond side of their respective minima (see Figure 5). Both populations will evolve in time, predominantly toward their potential minima. Directly after the pump, before these populations have shifted, the probe will see a bleaching signal due to the ground-state depletion. The time evolution of the particle and hole distributions is such that the $0 \rightarrow 1$ bleaching will shift away from the probe frequency, while the $1 \rightarrow 2$ absorption moves toward the probe frequency. Both processes result in a decrease of the bleaching signal. As the excitation itself will decay, giving rise to a temperature increase, the absorption change will reach its new equilibrium value. Between the last two counteracting processes, a minimum in the absorption change is reached.

In Figure 4c, the pump frequency is relatively blue. Therefore, the induced absorption initially is blue as well, dominating a short time over the bleaching signal. As the "holes" drift into the spectral window of the probe, the bleaching takes over, and the absorption change changes sign. The bleaching finally decays to an equilibrium value corresponding to a (locally) higher temperature of the sample.

5. Discussion

The observed lifetime of 1.8 ps of the OD stretch vibration of HDO:D_2O is in good agreement with the value of approximately 2 ps found for the lifetime of the OD stretch in pure D_2O.[14] The similarity of these numbers for the pure liquid and the isotopically diluted solution is quite surprising, since for the OH stretch vibration, the lifetime in pure H_2O is much shorter than in the diluted solution: ~200 fs versus 740 fs.[21] This difference is caused by the fact that in pure H_2O, where the distance between adjacent OH groups is small, the energy of an OH oscillator is rapidly transferred to nearby oscillators. This Förster energy transfer causes very fast spectral diffusion, and enables the vibration to find its most efficient relaxation path. Comparison of the OD stretch lifetime in HDO:H_2O (this study) and in pure D_2O[14] thus seems to indicate that intermolecular energy transfer plays a much smaller role for the OD stretching vibration than for the OH stretch. The somewhat smaller transition dipole moment of the OD stretch may at least partly explain the difference between water and deuterated water in Förster energy transfer rates.

It is an interesting observation that the lifetime of the OD stretch is more than twice as long as the OH stretch lifetime, since this conflicts with the energy gap law,[22] which states that the vibrational lifetime is proportional to δ^N, where $d \ll 1$ and N is the number of quanta dissipated in a particular accepting mode. For a lower-frequency vibration (e.g., the OD stretch compared to the OH stretch), N will in general be smaller, implying a shorter lifetime. In this case, however, the lower-frequency vibration lives *longer* than the higher-frequency vibration. It should be noted that, in addition to energy gap considerations, there are several other effects that determine the isotope effect in the vibrational lifetime, such as coupling strengths and the density-of-states of combined accepting modes.

In most vibrational relaxation processes, the energy is not transferred to a single accepting mode, but rather to a combination of modes, that may consist of one high-frequency mode that accepts the major part of the energy (such as the bending mode, ~1450 cm^{-1}) and several low-frequency modes to

compensate the energy difference, or many low-frequency modes (e.g., the hydrogen-bond mode $\sim$200 cm^{-1}). For high-frequency vibrations in the condensed phase, there are many combinations of accepting modes that match the energy to be dissipated and that are anharmonically coupled to the excited vibration. Hence, the relaxation rate will increase when the density of states of these combinations at the excitation energy increases.

For zeolites,[23] it was found that an OD stretch mode relaxes about three time as fast as an OH mode. From the temperature dependence of the vibrational lifetime, the numbers of quanta of accepting modes were determined to be 5 and 3, respectively. The energy gap law would predict a much larger difference in lifetime than the observed factor of 3. This relatively small difference could be explained from the difference in the number of accepting mode combinations, which was shown to be larger for the OH stretch vibration.

The isotope effect in the lifetime of the OH/OD stretching vibration can be understood by a similar argument: for isotopically diluted liquid water, apparently, the number of accepting modes is sufficiently larger for the OH stretching mode in HDO:D_2O than for the OD stretch of HDO:H_2O, that the OH stretch lifetime becomes shorter than the OD stretch lifetime, despite the larger energy gap.

It is not yet clear which are the accepting modes in the relaxation of an excited OD or OH stretching vibration. Two likely accepting modes are the HOD bending vibration, and the hydrogen-bond mode. Nienhuys et al.[12] found that the temperature and frequency dependence can be well explained if the relaxation involves energy transfer to the hydrogen bond. Deàk et al. found that the energy relaxation of both the OH and OD stretch modes leads to a transient excitation of the bending mode. Unfortunately, in the present experiments, we are not able to determine the precise relaxation mechanism. Probably, both the HOD bending mode and the hydrogen-bond mode play a role in the relaxation scheme.

For liquid water, values for the spectral diffusion correlation time have been obtained of 500 fs[16] and 700 fs.[11] In these studies, the OH stretching vibration was studied in a dilute solution of HDO in D_2O. As the frequency of the OH vibration is determined by the length of the hydrogen bond that binds the hydrogen atom to the oxygen atom of a nearby water molecule,[18] its dynamics result from the motion of the bulk D_2O molecules. In the present experiment, we studied the OD stretching vibration in a dilute solution of HDO in H_2O. The value for the spectral diffusion time of 400 fs directly reflects the motion of H_2O molecules. In measuring this value, the OD excitation serves only as a label to follow the spectral dynamics. The fact that the vibrational lifetime is a few times as large as the spectral diffusion correlation time, allows for a very precise determination of the latter value. The shorter spectral diffusion time implies that H_2O molecules show significantly faster hydrogen-bond dynamics than D_2O.

6. Conclusions

We performed two-color mid-infrared pump−probe experiments on the OD stretching vibration in HDO:H_2O. The data could be very well modeled using the Brownian oscillator model. From this model, the vibrational lifetime and the spectral diffusion time have been determined; their values are 1.8 ps and 400 fs, respectively. The vibrational lifetime of the OD stretching vibration is found to be significantly longer than that of the OH stretching vibration. The spectral diffusion correlation time is shorter than previously obtained for D_2O, which means that the hydrogen-bond dynamics is faster in H_2O than in D_2O.

Acknowledgment. This work is part of the research program of the Stichting Fundamenteel Onderzoek der Materie (Foundation for Fundamental Research on Matter) with financial support from the Nederlandse Organisatie voor Wetenschappelijk Onderzoek (Netherlands Organization for the Advancement of Scientific Research).

References and Notes

(1) Wyss, H. R.; Falk, M. *Can. J. Chem.* **1970**, *48*, 607.
(2) Ford, T. A.; Falk, M. *Can. J. Chem.* **1968**, *46*, 3579.
(3) Herzberg, G. *Molecular spectra and molecular structure*; D. van Nostrand: New York, 1950.
(4) Boyd, T. A. *Nonlinear Optics*; Academic Press: London, 1992.
(5) Laubereau, A.; Greiter, L.; Kaiser, W. *Appl. Phys. Lett.* **1974**, *25*, 87.
(6) Knudtson, J. T.; Stephenson, J. C. *Chem. Phys. Lett.* **1984**, *107*, 385.
(7) Bakker, H. J.; Planken, P. C. M.; Kuipers, L.; Lagendijk, A. *J. Chem. Phys.* **1991**, *94*, 1736.
(8) Graener, H.; Ye, T. Q.; Laubereau, A. *J. Chem. Phys.* **1988**, *90*, 3413.
(9) Woutersen, S.; Emmerichs, U.; Bakker, H. J. *Science* **1997**, *278*, 658.
(10) Laenen, R.; Rauscher, C.; Laubereau, A. *Phys. Rev. Lett.* **1998**, *80*, 2622.
(11) Gale, G. M.; Gallot, G.; Hache, F.; Lascoux, N.; Bratos, S.; Leicknam, J.-C. *Phys. Rev. Lett.* **1999**, *82*, 1068.
(12) Nienhuys, H. K.; Woutersen, S.; van Santen, R. A.; Bakker, H. J. *J. Chem. Phys.* **1999**, *111* (4), 1494.
(13) Woutersen, S.; Bakker, H. J. *Nature* **2000**, *402*, 507.
(14) Deàk, J. C.; Rhea, S. T.; Iwaki, L. K.; Dlott, D. D. *J. Phys. Chem. A* **2000**, *104*, 4866.
(15) Woutersen, S.; Emmerichs, U.; Bakker, H. J. *J. Chem. Phys.* **1997**, *107*, 1483.
(16) Woutersen, S.; Bakker, H. J. *Phys. Rev. Lett.* **1999**, *83*, 2077.
(17) Franks, F. *Water*; Royal Society of Chemistry: London, 1983.
(18) Mikenda, W. *J. Mol. Struct.* **1986**, *147*, 1.
(19) Mukamel, S. *Nonlinear optical spectroscopy*; Oxford University Press: New York, 1995.
(20) Yan, Y. J.; Mukamel, S. *Phys. Rev. A* **1990**, *41*, 6485.
(21) Lock, A. J.; Woutersen, S.; Bakker, H. J. *J. Phys. Chem. A* **2001**, *105*, 1238.
(22) Nitzan, A.; Mukamel, S.; Jortner, J. *J. Chem. Phys.* **1975**, *63*, 200.
(23) Brugmans, M. J. P.; Bonn, M.; Bakker, H. J.; Lagendijk, A. *Chem. Phys.* **1995**, *201*, 215.